Development and parameter estimation of snow-melt models using spatial snow-cover observations from MODIS

Dhiraj Raj Gyawali and András Bárdossy

Institute for Modelling Hydraulic and Environmental Systems (IWS), University of Stuttgart

Correspondence: Dhiraj Raj Gyawali (dhiraj.gyawali@iws.uni-stuttgart.de)

Abstract. Given the importance of snow on different land and atmospheric processes, accurate representation of seasonal snow evolution including distribution and melt volume, is highly imperative to any water resources development trajectories. The limitation of reliable snow-melt estimation in the mountainous regions~~these regions~~ is however, further exacerbated with data scarcity. This study attempts to develop relatively simple ~~r~~ extended degree-day snow-models driven by freely available snow cover images ~~in snow-dominated regions~~. This approach offers relative simplicity and plausible alternative to data intensive models as well as in-situ measurements and have a wide scale applicability, allowing immediate verification with point measurements.

The methodology employs readily available MODIS composite images to calibrate the snow-melt models on spatial snow-distribution in contrast to the traditional snow-water equivalent based calibration. The spatial distribution of snow cover is simulated using different extended degree-day models with parameters calibrated against individual MODIS snow-cover images for cloud-free days or a set of images representing a period within the snow season. The study was carried out in Baden-Württemberg in Germany, and in Switzerland. The simulated snow cover show very good agreement with MODIS snow cover distribution and the calibrated parameters exhibit relative stability across the time domain.

The melt from these calibrated snow-models were used as standalone inputs to a modified HBV without the snow component in all the study catchments~~The snow-melt from these calibrated snow-models were used as standalone inputs to a 'truncated HBV' without the snow component in Reuss (Switzerland), and Horb and Neckar (Baden-Württemberg) catchments~~, to assess the performance of the melt outputs in comparison to a calibrated standard HBV model. The results show an overall increase in NSE performance and a reduction in uncertainty in terms of model performance. This can be attributed to the reduction in the number of parameters available for calibration in the modified HBV, and an added reliability of the snow accumulation and melt processes inherent in the MODIS calibrated snow-model output. ~~The results further show slight increase in overall NSE performance and a better NSE performance during the winter. Furthermore, 3-15% decrease in mean squared error was observed for the catchments in comparison to the results from standard HBV. The increased NSE performance, albeit less, can be attributed to the added reliability of snow-distribution coming from the MODIS calibrated outputs.~~

This paper highlights that the calibration using readily available images used in this method allows a flexible regional calibration of snow cover distribution in mountainous areas ~~across a wide geographical extent~~ with reasonably accurate precipitation and temperature data and globally available inputs. Likewise, the study concludes that simpler specific alterations to processes contributing to snow-melt can contribute to reliably identify the snow-distribution and bring about improvements

in hydrological simulations owing to better representation of the snow processes~~to some extent the flows~~ in snow-dominated regimes.

1 Introduction

Reliable representations of spatial distribution of seasonal snow and subsequent snow-melt are critical challenges for hydrological estimations, given their crucial relevance in mountainous regimes especially because of the high sensitivity to climate change. Considering the snow effect on land and atmospheric processes, accurate representation of seasonal snow evolution is thus highly imperative to strengthen water resources development trajectories in these regions (Kirkham et al., 2019; Schmucki et al., 2014; He et al., 2014). Various modeling and measurement techniques are currently in practice which attempt to estimate ~~this~~ distribution of snow but these methods hold their own limitations. Prior studies on the comparison of snow models (Feng et al., 2008; Rutter et al., 2009) have highlighted the higher reliability of physically based approaches such as the energy balance approach~~complex models~~ in simulating the snow conditions. However, depending upon the complexities of the models, there exist big differences in model results. These complex models, though offer a more realistic physical detail of the sub-processes (Wagner et al., 2009), are often associated with intensive data requirement, which is generally a big limitation in mountainous catchments around the world (Girons Lopez et al., 2020).~~Relatively accurate physically based models are highly data intensive, which is mostly a big limitation in mountainous catchments around the world.~~ Likewise, in-situ measurements of snow-depth providing accurate measure~~s of snow depth can~~ seldom cover a wider spatial extent and are prone to be non-representative due to local influences. Lack of snow-depth information and to some extent, persistent cloud cover in the mountains limit the standalone usage of Remote sensing images in snow estimation (Tran et al., 2019). However, these images can provide a plausible alternative to ground based data especially in the data scarce mountainous~~mountain~~ regions, since their resolution and availability do not depend on the ~~mountainous~~ terrain (Parajka and Blöschl, 2008).

The MODerate resolution Image Spectralradiometer (MODIS) (Hall et al., 2006) on board Terra and Aqua satellites provide are the~~one~~ of the most extensively used snow cover products worldwide ~~for snow cover monitoring~~ owing to their daily temporal resolution and a high spatial resolution of 500m at the Equator. The MODIS snow-cover data performance, though seasonally and region dependent, has been found to be accurate enough for hydrological context (Parajka and Blöschl, 2008). The cloud obstruction in MODIS, though significant, can be reduced combining the Aqua and Terra MODIS images and other spatio-temporal filtering techniques (Tran et al., 2019; Gafurov and Bárdossy, 2009; Wang and Xie, 2009).

Remote sensing integration in hydrological modeling has gained important strides in the recent years (Wagner et al., 2009). Sirisena et al. (2020) used remote sensing-based evapotranspiration data along with discharge to calibrate hydrological models ~~a hydrological model~~ and concluded that the multi-variable calibration with globally available remote sensing data along with traditionally used discharge based calibration can lead to better representation of the hydrological processes, especially in data scarce regions. Sun et al. (2015) used satellite observations derived river width to calibrate a hydrological model in an ungauged basin leading to good agreement with monthly discharge data. Parajka et al. (2009) implemented a calibration for a conceptual hydrological model in Austria using ERS scatterometer derived surface soil moisture data and discharge. They concluded that

the combined use of discharge and soil moisture improves the simulation of soil moisture while maintaining the discharge performance of the model. They further discussed that the augmentation of satellite data allows for a more robust parameter estimation. Parajka and Blöschl (2008) implemented a snow-cover (MODIS) and discharge constrained calibration to simulate flows in 148 catchments in Austria and concluded that this multi-objective calibration scheme improved the snow-model

65 performance though the overall performance of the hydrological model was similar. MODIS snow-cover was used by (He et al., 2014) to estimate distributed degree-day factors for snow-melt modeling. Udnæs et al. (2007) discussed the operational application of MODIS SCA in the Hydrologiska Byråns Vattenbalansavdelning (HBV) (Bergström, 1995) model for spring flood prediction. They concluded that the combined calibration with SCA and discharge resulted in better prediction of the snow cover distribution, albeit a similar performance with discharge. Tekeli et al. (2005) used MODIS products in identifying

70 the snow duration curve to be used in a snow-melt model and concluded that the coupling provides crucial information on snow-melt timing and magnitude. Likewise, there have been many studies to compare and improve the snow routine in various hydrological models in recent years. Girons Lopez et al. (2020) evaluated various formulations of the temperature-index approach to analyze their response via the HBV model in 54 mountainous European catchments. They concluded that these specific targeted alterations improve the performance in terms of snow processes. Caicedo et al. (2012) also identified the best

75 performing variants of degree-day calculations for different regions in Colombia.

~~Simple distributed snow-melt modeling approaches incorporating readily available meteorological data and these cloud filtered remote sensing images can be used to estimate the spatial extent that are free from highly localized influences. These simpler models offer a wide scale applicability and allow immediate verification with point measurements and this holds a high relevance in data scarce regions.~~

80 T~~Against this backdrop, t~~his work aims to implement a methodology using MODIS snow-cover images to identify and to calibrate different variants of melt models to estimate a time-continuous spatial snow extent in snow dominated regimes. The assimilation of the cloud filtered remote sensing images with the simple but widely used distributed temperature index snow-melt modeling approaches can be pivotal in estimating the spatial extent of snow cover that are free from highly localized influences. Widely used and computationally simplistic temperature index models with low data requirement are considered

85 in the study and are modified wherever possible, to gain enhanced model performance. These simpler models assimilated with remotely sensed snow-cover data, offer a wide scale applicability, allow immediate verification with point measurements and hold a high relevance in data scarce regions. Modifications to the models in this study, include a simple degree-day model followed by incorporation of different aspects governing snow hydrology such as precipitation induced melt, radiation, topography, and land use.

90 The main objective of this research study is to develop a flexible snow-melt module useful for distributed hydrologic modeling, applicable in mountainous regimes across a wide geographical extent, with parameters which can be estimated by MODIS or other satellite-based snow cover products. The novelty of this research is the independent calibration of the snow-melt models on snow-cover images which allows quick and standalone estimation of parameters associated with and a better representation of the snow processes. The calibration using snow-cover distribution, offers adequate spatial flexibility and computational

95 efficiency, albeit the simplicity, to calibrate melt models on an individual or a set of images and estimate the snow distri-

bution in mountainous areas across different regions with reasonably accurate precipitation and temperature data. This also identifies more robust parameter sets as the model uncertainty related to snow processes is significantly reduced. In addition, the melt simulated by the snow-melt models can be coupled with hydrological models to improve the discharge prediction. This allows for a simpler calibration of the hydrological models as there are less parameters to be estimated~~optimized~~. Furthermore, the equifinality is a well-known challenge in hydrological modeling (Beven, 2001). This approach tends to reduce the hydrological model uncertainty as the set of equifinal parameters becomes smaller. ~~The main objective of this research is to develop a flexible snow-melt modules useful for distributed hydrologic modeling, applicable in mountainous regimes across a wide geographical extent, with parameters which can be estimated by MODIS or other satellite-based snow cover products. Furthermore, calibration using readily available images proposed in this method, offers adequate flexibility and computational efficiency, albeit the simplicity, to calibrate melt models on an individual or a set of images and estimate the snow distribution in mountainous areas across different regions with reasonable precipitation and temperature data. This study intends to obtain a time continuous spatial snow cover and resulting melt which can be as a stand-alone input, coupled with distributed hydrological models to improve the model predictions.~~

The paper is organized as follows. After a brief introduction section, the study area and the spatio-temporal data used are explained. The following section then details the methodological framework including degree-day models and the calibration and validation approach used in the study. The result section discusses the study findings in terms of calibration and validation results at regional level, spatio-temporal transferability of parameters, model validation at catchment levels, and the validation of the melt model outputs in the hydrological models. The final section discusses the results and outlines the concluding remarks of the study.

2   Study Area and Data

To develop and test simple snow models in the mountainous / snow dominated regions, the study area is ~~As explained above, this study attempts to test the efficacy of the aforementioned approach in the mountainous / snow dominated regimes. The study area is, thus~~ selected as two distinct snow-regimes, a) characterized by intermittent snow and b) characterized by partly longer duration snow. For the former, Baden-Württemberg (BW) region in Germany was selected. Whole of Switzerland was considered to represent the longer~~long~~ duration snow for the study. Figure 1 below shows the study domain~~area~~:

The BW region includes the Schwabian Alps with the elevation rising to 1465 masl from a lowest of 88 masl. Likewise, Switzerland includes the Swiss Alps region which covers the perennial snow/glacier area. The elevation ranges from below 200 to 4448~~4415~~ masl. The study areas exhibit an average snow season from October to April in Germany and September to June in Switzerland. For hydrological modeling, five catchments, viz, Neckar catchment at Rottweil and Horb in BW, and Reuss catchment at Seedorf, Aare catchment at Brienzwiler and Thur catchment at Andelfingen in Switzerland, were selected. The Reuss and Aare catchments have a longer snow-cover around the year and include glaciated areas. The properties of the catchments are shown below in Table 1.

~~3. Data and sources~~
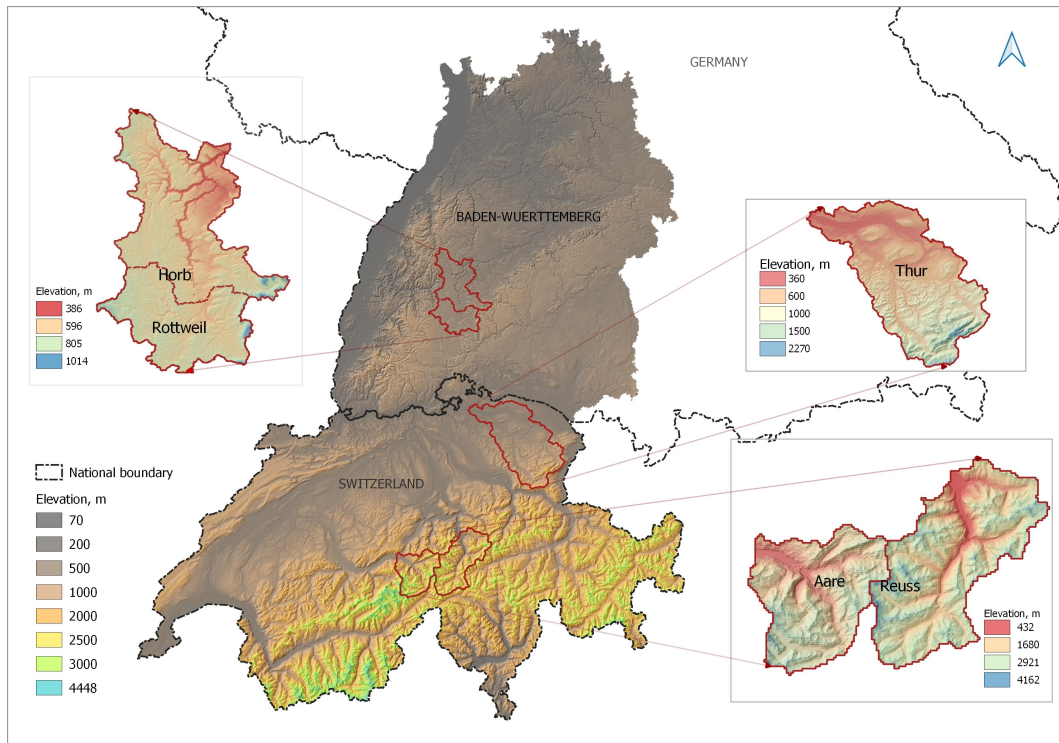
Figure 1. Map of the study area with elevation

Table 1. Catchment properties

River	Outlet	Catchment Area, sq.kms	Catchment Elevation, masl			Glaciation,%
			Max	Min	Mean	
Neckar	Rottweil	412	1006	555	705	0
Neckar	Horb	1110	1006	386	656	0
Reuss	Seedorf	837	3416	437	2010	6.4
Thur	Andelfingen	1702	2217	372	770	0
Aare	Brienzwiler	555	3798	580	2135	15.5

The data used for the study are ~~as briefly discussed as follows~~:

130   – **Hydro-meteorology** : Daily station meteorological data viz. precipitation, and minimum, maximum and mean temperatures from 2010-2018 were acquired for the study. For Germany, these variables were obtained from the Deutsche Wetterdienst (DWD),~~whereas for Switzerland the data was collected~~ and from Federal Office of Meteorology and Climatology (MeteoSwiss) for Switzerland. Likewise daily discharge timeseries for selected catchments were acquired

collected to validate the efficacy of the approach in HBV model, from Bundesanstalt für Gewässerkunde (BFG) for

135   Germany and Federal Office for the Environment (FOEN) for Switzerland.

– **Topography**: Shuttle Radiation Topography Mission (SRTM) 90m resolution Digital Elevation Model (DEM) (Jarvis et al., 2008) was used in the study. The DEM was rescaled to match the MODIS resolution for consistency. Likewise, aspect and slope rasters were also obtained from this DEM.

– **Snow-cover**: Daily MODIS Terra and Aqua snow-cover dataSnow Cover products Version 6 (Hall and Riggs, 2016)

140   from 2010 to 2018 were used for calibrating the models and further analysis of snow distribution in the study regions. The resolution of the data is 500m at the Equator and 464m in the study region.

4. Data preparation This study presents a distributed modeling approach with model computations done at pixel level of a gridded domain of 464m x 464m grids. For this, the input data were pre-processed and interpolated onto the aforementioned grid cellsceellls. Following sequential steps were adopted for the data preparation.

145   4.1 Schema extraction

A gridded 464mx464m schema was extracted for both regions using the MODIS snow cover data as a reference. This schema was considered as the reference gridded domain for the data interpolation and model run.

2.1   MODIS pre-processing **and cloud removal**

The Aqua and Terra variants of MODIS snow cover data were downloaded and then pre-processed. in different steps, viz.

150 mosaicking, reprojection and clipping, using the GDAL module in Python. For uniformity, WGS84 UTM 32N was used as the base projection system. 4.2 Cloud removal The pre-processed MODIS images were sequentially and spatio-temporally filtered using a cloud-removal procedure as described in Gafurov and Bárdossy (2009). The procedure follows the following steps below:

(a) The first step checks the Aqua-Terra image combination. Pixels with clouds (255) in one of the images and land (0) or

155   snow (1-100) in the other was replaced with the snow / land value and vice versa. The output is a combined raster with reduced cloud pixels. The combined raster was then reclassified as ‚0‘ and ‚1‘. No snow pixel values of the combined raster (0) are set to ‚0‘ and snow pixel values (1-100) are set to ‚1‘. Everything else is set to ‘No data’.

(b) The second step compares the preceding and succeeding days for a pixel under consideration. If both the days for the pixels are cloud-free with 0 or 1, the pixel under consideration will respectively get either 0 or 1 for the day.

160 (c) Likewise the third step compares two days backward and one day forward, and one day backward and two days forward combination to check for the cloud free days and infill accordingly, assuming consecutive snow or no-snow days.

(d) The fourth step compares the lowest elevation with snow and the highest elevation without snow for each day. Any pixel with elevation higher than the lowest elevation snow pixel would get ‚1‘ and the elevation lower than the highest elevation without snow would get ‚0‘.

165   (e) The fifth step searches for '0' or '1' in a 8 pixel neighbourhood surrounding the cell. If the neighbourhood has a mode
       at least 4 valid values, the pixel will then be either '0' or '1'.

2.2   Spatial interpolation of precipitation and temperature

Both BW and Switzerland have a well distributed and dense network of meteorological stations. ~~Figure 2 below shows the~~
~~precipitation station network in Switzerland.~~ The daily precipitation and temperature values from these stations were used for
170 geostatistical interpolation onto the aforementioned schema for the regions. ~~The Kriging process used are explained further in~~
~~the following section.~~
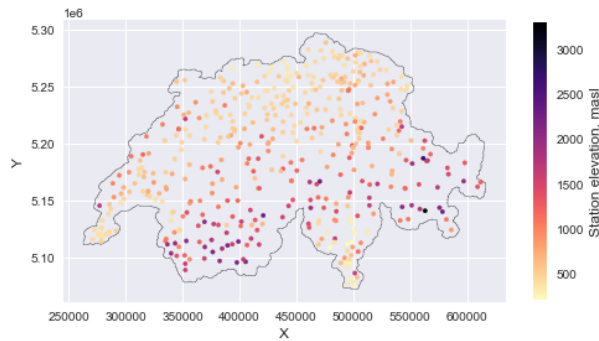
Figure 2. ~~Precipitation station network in Switzerland~~

~~4.2.1 Daily temperature interpolation~~

For the interpolation of temperature data, External Drift Kriging (EKD) was opted in the regions under study, with station
elevation as a drift (Hudson and Wackernagel, 1994). The station elevation exhibits strong correlation with the monthly and
175 seasonal temperatures. Daily minimum, maximum and mean temperatures from 85 stations in Baden-Württemberg and 365
stations for Switzerland were used for the interpolation. Cross validation using leave-one-out approach was carried out to check
for the applicability and the quality of the EKD interpolation.

~~4.2.2 Daily precipitation interpolation~~

For precipitation, the~~The~~ daily precipitation sums were interpolated onto the schema using a detrended Residual Kriging
180 (RK) (Phillips et al., 1992; Martínez-Cob, 1996). To improve the precipitation interpolation in the higher elevation, a multiple
linear regression (MLR) approach using directionally smoothed elevation was carried out for the study. Directional smoothing
of elevation was done using half-space smoothing (Bárdossy and Pegram, 2013). The approach uses a directionally transformed
and smoothed topography to identify the effect of directional advection for each day. Eight different directions with 45 degrees
incremental angles, and 3 different smoothing distances (2, 3 and 5 kms) were considered in this study. For each time-step, a
185 simple optimization was done to assess the correlation of the precipitation with the shifted DEMs, and the best direction and
the smoothing radius for the timestep were identified. This shifted and smoothed elevation was then used along with X and
Y coordinates of the stations in the MLR to obtain precipitation estimates for stations. The residuals were then calculated for

each day and ordinary Kriging was carried out to obtain the Kriged residuals. MLR estimated precipitation surfaces for each time step using X and Y coordinates and shifted elevation for the grid points were then added to the Kriged residual surfaces

190 to obtain the final precipitation estimates. 224 stations in BW, and 449 stations in Switzerland were used in this study. Leave-one-out cross validation for each station was done for both variables. ~~and the rainfall and temperature Kriging performance was evaluated using Nash-Sutcliffe Efficiency (NSE, Eq. (1)~~ for each station.

$$NSE = 1 - \frac{\sum_{t=1}^{T} \left(Y_o^t - Y_m^t \right)^2}{\sum_{t=1}^{T} \left(Y_o^t - \bar{Y}_o^T \right)^2}$$

~~Where,~~

~~Y_m^t = Simulated ('Kriged') variable at time t,~~

195 ~~Y_o^t = Observed variable at time t,~~

~~$\bar{Y}_o^T$ = mean of observed variable for the time period T,~~

~~T = length of timeseries,~~

3   Methodology ~~Framework~~

The methodological framework applied for the study is shown below in Fig. 3 and is further discussed in subsequent sections.
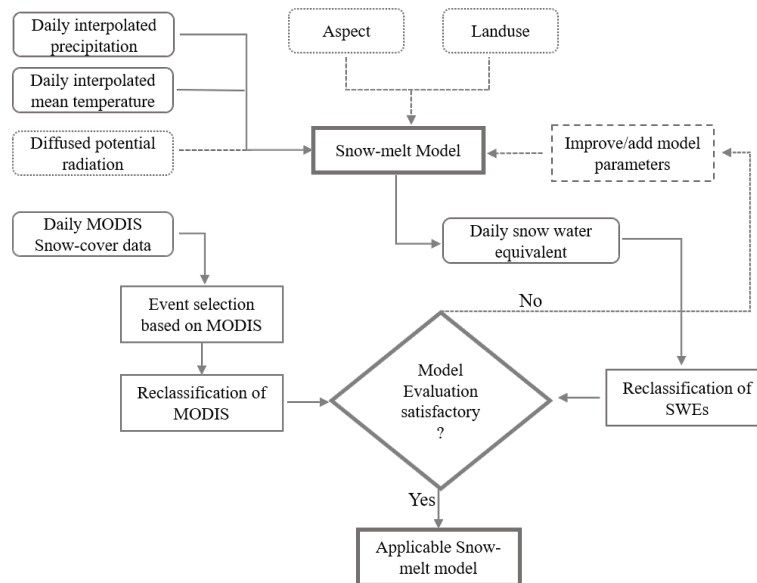
Figure 3. Methodological approach for the study

200 ~~6. snow-melt models~~

This study employs empirical, temperature-index melt modelling approach using the degree day factors. The degree day models are widely used owing to relatively easier interpolation of air temperature, and reasonable computational simplicity (Hock, 2003). This degree-day approach assumes melt rate as a linear function of the air temperature. Due to inherent large-scale spatial variability in the mountain regions, distributed meteorological inputs, were employed to drive the different variants of the extended degree-day snow-melt models on a daily timescale. The major parameters used in the models are defined below.

Where,

$P(t,x)$= precipitation amount at location x at time t, mm

$S(t,x)$= snow water equivalent amount at location x at time t, mm

$T_{av}(t,x)$= mean temperature at location x at time t, °C

$P_s(t,x)$ = water equivalent of precipitation falling as snow at location x at time t, mm

$M_s(t,x)$ = melt water amount at location x at time t, mm

T_T = threshold critical temperature defining snow or no snow, °C

D_s = dry degree day factor, $mm°C^{-1}$

$T_{mx}(t,x)$= maximum temperature at location x at time t, °C

$T_{mn}(t,x)$= minimum temperature at location x at time t, °C

scf= snow correction factor to account for the gauge undercatch of snow

The following model variants were used to estimate the snow-water equivalent (SWE, mm) and the resulting snow cover in each pixel. Different nomenclatures are given to the models for the ease of understanding. Each successive model represents a gradual parameter wise modification to the basic degree-day model.

Basic Degree-day Model (Model 1)

Model 1This model is the most basic of all model variants and is also used in the HBV model. This model estimates the melt for each time-step as a linear function of the difference between daily mean temperatures and a threshold temperature value demarcating liquid precipitation and snow precipitation. A degree day factor controls the rate of melt. Equation (1) calculates the amount of SWE available in pixel 'x' at time 't'. Similarly the snow-precipitation and the resulting melt are calculated with Eq.(2) as the model basis for each pixel, 'x' in the study domain. A correction factor to account for the snowfall undercatch by the gauges and the vegetation interception scf is also used in this model and extended to all models in the study.

$$S(t,x) = S(t-1,x) + P_s(t,x) - M_s(t,x), \tag{1}$$

Where,

$$P_s(t,x) = \begin{cases} P(t,x) \cdot scf & \text{if } T_{av}(t,x) < T_T \\ 0 & \text{if } T_{av}(t,x) \geq T_T \end{cases} \tag{2a}$$

$$M_s\left(t,x\right) = \begin{cases} 0 & \text{if } \ T_{av}(t,x) < T_T \\ min(S\left(t,x\right), \ \ D_s \ (T_{av}\left(t,x\right) - T_T) & \text{if } \ T_{av}(t,x) \geq T_T \end{cases} \tag{2b}$$

Wet Degree-day Model (Model 2)

To account for the melt induced by rain at temperatures higher than the critical threshold temperature, this variant adds a precipitation melt factor which controls the rate of melt based on air temperature and the precipitation amount falling on the pack. Similar approach was discussed in Bárdossy et al. (2020).~~In addition to the temperature induced melt, this variant adds melt due to liquid water falling on the snowpack.~~ This melt factor, henceforth referred to as D_w increases the melt from Eq.(2b) on days with precipitation higher than a threshold value. For a given wet day i.e., $P(t,x) > P_T$, the melt is calculated as in Eq.(3). For a dry day, melt is calculated as Eq.(2b).

$$M_s\left(t,x\right) = \begin{cases} 0 & \text{if } \ T_{av}(t,x) < T_T \\ min(S\left(t,x\right), \ \ D(t,x) \ (T_{av}\left(t,x\right) - T_T) & \text{if } \ T_{av}(t,x) \geq T_T \end{cases} \tag{3}$$

Where,

$D(t,x) = D_s + D_w(P(t,x)$ - $P_T)$

P_T = Threshold precipitation depth beyond which the liquid precipitation contributes to melt, mm

D_w = the wet melt factor, $mm.mm°C^{-1}$

$D(t,x)$ = combined melt factor on wet days, $mm°C^{-1}$

Wet Degree-day Model with snowfall and snow-melt temperatures (Model 3)

The instantaneous forms of precipitation as snow and liquid gives a clear indication of two temperature thresholds which demarcate the solid and liquid state of precipitation (Schaefli et al., 2005). This model includes different snowfall and snow-melt temperatures in Model 2 for a more accurate representation of the liquid to snow phase partition and melt initiation. This has been previously discussed in (Debele et al., 2009; Girons Lopez et al., 2020). For temperatures in between, snow is linearly interpolated for the day as a proportion of the precipitation. The formulation of the model are given by Eqs.(4) and (5).

$$P_s\left(t,x\right) = \begin{cases} P\left(t,x\right) & \text{if } \ T_{av}(t,x) < T_S \\ P\left(t,x\right) \cdot \left(\frac{T_{av}(t,x)-T_M}{T_S - T_{av}(t,x)}\right) & \text{if } \ T_S \leq T_{av}(t,x) \leq T_M \\ 0 & \text{if } \ T_{av}(t,x) > T_M \end{cases} \tag{4}$$

$$M_s(t,x) = \begin{cases} 0 & \text{if} \quad T_{av}(t,x) < T_M \\ min(S(t,x), \quad D(t,x) \ (T_{av}(t,x) - T_M)) & \text{if} \quad T_{av}(t,x) \geq T_M \end{cases} \tag{5}$$

Where,

T_S and T_M are the snowfall and snow-melt temperatures respectively.

Aspect distributed snowfall temperatures (Model 4)

This model was envisioned with an assumption that topographical aspect plays a major part in the spatial distribution of snowfall and snow-melt temperatures. In general, south facing slopes are warmer in the Northern hemisphere resulting in a faster melt of snow compared to the north facing slopes. Based on this assumption, this variant distributes the snowfall temperature in Model 3, according to the topographical aspect. The snowfall temperature distribution is done by Eq.(6) below:

$$T_{S,x} = T_{Smin} + (T_{Smax} - T_{Smin}) * [0.5 * \cos(aspect_x) + 1]^{PF} \tag{6}$$

Where,

T_{Smin} = lower bound of the snowfall temperature

T_{Smax} = upper bound of the snowfall temperature

$aspect_x$ = topographical aspect of grid 'x', (radians)

PF = power factor to distribute the aspect

Aspect distributed snow-melt temperatures (Model 5)

This model distributes the snow-melt temperature in Model 3 within a range defined by minimum and maximum snowfall temperature, according to the topographical aspect. The snow-melt distribution is represented by Eq.(7) below:

$$T_{M,x} = T_{Mmin} + (T_{Mmax} - T_{Mmin}) * [0.5 * \cos(aspect_x) + 1]^{PF} \tag{7}$$

Where,

T_{Mmin} = lower bound of the snowfall temperature

T_{Mmax} = upper bound of the snowfall temperature

$aspect_x$ = topographical aspect of grid 'x', (radians)

PF = power factor to distribute the aspect

Radiation Induced melt Model (Model 6)

The integration of radiation information in degree-day models can lead to better estimation of snow-melt (Hock, 2003). This model was formulated to accommodate the radiation data in addition to the aspect-based temperature distribution. The radiation induced melt was added to~~adds radiation induced melt to~~ Model 5 by incorporating the diffused incident radiation on the snow pixel on a cloud-free day. The incident global radiation is calculated using a viewshed based algorithm "r.sun algorithm" (Hofierka and Suri, 2002; Neteler and Mitasova, 2002) and has an added advantage of radiation distribution in the valleys. Daily temperature difference (tmax -tmin) for each grids was also calculated using interpolated daily minimum and maximum temperatures and was used as a cloud cover proxy. For this study, pixels with a daily temperature difference above a certain threshold were assumed to be cloud free and this is where radiation induced melt became active. Likewise, temperature differences lesser than the threshold render the pixels cloudy. The diffusion factor ranging from 0.2 for clear sky conditions to 0.8 for overcast conditions diffuses the incoming radiation. The radiation induced melt is added to the melt outputs from the preceding models on cloud-free~~cloudlfree~~ pixels and is calculated using Eq.(8). Figure 4 below shows an example of diffused radiation calculated for a cloud free day in Baden-Württemberg.

$$
M_{s-R}(t,x) = \begin{cases} (1-alb)\cdot r_{ind}\cdot R_D(t,x) & \text{if} \quad T_{mx}(t,x) - T_{mn}(t,x) \geq 5°\text{C} \\ 0 & \text{if} \quad T_{mx}(t,x) - T_{mn}(t,x) < 5°\text{C} \end{cases} \tag{8}
$$

Where,

$M_{s-R}(t,x)$ = Radiation induced melt at grid x at time t, mm

$R_D(t,x)$ = Diffused radiation at gird x at time t, $Wh\cdot m^{-2}day^{-1}$

alb = Albedo of snow

r_{ind} = Radiation melt factor, $mm\cdot(Wh.m^{-2}day^{-1})$

$(T_{mx}(t,x) - T_{mn}(t,x))$ = temperature difference at time t, as a cloud proxy to define clear-sky and overcast conditions

3.1 Data requirement of the models

Table 2 below summarizes the input data requirement for each model ~~indicating both spatial and temporal resolution~~. The major inputs are the DEM, precipitatiton and temperature data. The other variables are the derivatives from these major inputs. For instance, daily temperature difference was considered as a proxy for the cloud information. The aspect information and daily global radiation are derived from the DEMs. In addition to the data presented in the table, the daily MODIS snow-cover distribution is also required for model calibration and evaluation. Freely available inputs such as the DEM and the MODIS images provide a crucial flexibility with minimum data requirement to drive the snow-melt models. Likewise, daily observed stream-flows are also used~~required~~ for calibration and validation of the HBV model.
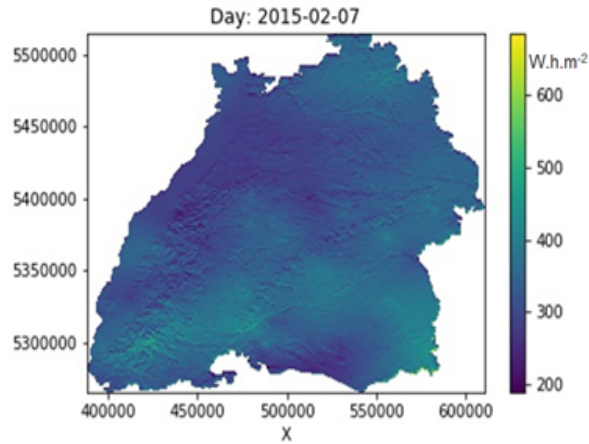
Figure 4. Illustration of diffused radiation calculated using r.sun.daily algorithm for Baden-Württemberg

Table 2. Inputs required for the different model variants

Models	Spatial inputs	Spatio-temporal inputs (daily)		
	DEM	**Precipitaion, mm**	**Mean Temp.,°C**	**Max. / Min Temp, °C**
Model 1	*yes*	*yes*	*yes*	-
Model 2	*yes*	*yes*	*yes*	-
Model 3	*yes*	*yes*	*yes*	-
Model 4	*yes*	*yes*	*yes*	-
Model 5	*yes*	*yes*	*yes*	-
Model 6	*yes*	*yes*	*yes*	*yes*

3.2 Model calibration

310 In order to calibrate the model parameters, the snow cover calculated by the snow model was compared to the MODIS observations on days with available data, A pixel was considered as snow covered if the snow water equivalent calculated was exceeding 0.5 mm which corresponds to a snow depth of approximately 2.5 mm

~~The snow-water equivalent (SWE, mm) obtained from the snow-models at each pixel were reclassified as '1' (snow) or '0' (no snow), thus simulating a snow-distribution pattern for the reference calibration event/duration. The reclassification was~~
315 ~~done based on a threshold level of 0.5mm (assuming a snowpack density of 20% ca.2.5mm of snow depth). The threshold depth was defined to ignore the transient snowfall events. Pixels with model-simulated SWE values greater than 0.5mm were considered as snowy pixels and values less than the threshold were considered pixels with no snow. Likewise, the MODIS images were also reclassified based on the snow proportion at each pixels. The pixel values from more than 0 to 100 were reclassified as '1' and the pixel values with'0' remain '0'. The rest of the values were reclassified as 'No Data' pixels and~~

320 ~~were not considered during the calibration. The reclassified MODIS image or a set of images with binary (0 or 1) values for a relatively cloud-free event or a duration during the winter was selected as the observed snow cover distribution for calibrating the models. The study employed a unique image-based pattern calibration approach in contrast to the more widely used calibration approaches using SWEs. As described in the previous section, the different extended degree-day models were calibrated on the reclassified MODIS-inferred snow cover distribution for a certain cloud-free day or for a duration within~~
325 ~~the snow season (eg. November-December) of a given year as observed reference. The major advantage of using image based calibration is the flexibility it offers to regionally calibrate the models on a single image for a certain cloud-free day, or on a set of images for a melt, onset season or even the whole time-series.~~

The calibration is based on the ~~used a simple~~ Brier-score (BS) ~~as the objective function~~ (Eq.(9)). It ~~The BS~~ is a score function that measures the accuracy of probabilistic predictions. ~~It can also be inferred as the mean squared error as applied~~
330 ~~to these predicted probabilities.~~ The BS in this study refers to the mean squared error between observed binary patterns of snow/no snow from MODIS and the ones simulated by the extended degree-day models. The Brier-score varies between 0 and 1 with the values closer to ,0' indicating better agreement between the model outputs and the MODIS image. ~~Once the parameters were estimated for the model, it was then validated for cloud free days in different years and seasons. This was repeated for different variants of snow models described in the above sections.~~

335
$$BS(t) = \frac{1}{N}\sum_{t=1}^{N}(f_i(t) - O_i(t))^2 \tag{9}$$

Where,

$f_i(t)$ = simulated snow cover (0/1) on day t and pixel i, $o_i(t)$ = observed snow cover (0/1) on day t and pixel i

The objective function is the sum of the BS values over the days with observed MODIS snow cover:

340
$$OF = \sum_{k=1}^{K}BS(t_k) \tag{10}$$

Where,

t_k are the days with observed MODIS snowcover,

The snow model parameters were identified by minimizing objective function (10). In order to reflect the equifinality of the model, the Robust Parameter Estimation (ROPE) (Bárdossy and Singh, 2008) methodology was applied for the model
345 parameter optimization. ROPE uses the concept of data depths to identify best-performing robust parameter sets and their properties for different calibration periods in different catchments, with an underlying assumption that it identifies parameters sets without overemphasizing the processes defined by the parameters. A set of 1000 heterogeneous parameter vectors with similar model performance in terms of the objective function were generated. These sets of 'good' points can be defined as the parameter sets that are less-sensitive and transferable, thereby providing a 'compromised' solution. ~~The Differential Evolution~~
350 ~~(DE) optimization scheme was considered in this study for the calibration process. The DE approach optimizes by iteratively trying to improve a candidate solution with regard to a given measure of quality. It provides a true global minimum of a multi~~

~~modal search space regardless of the initial parameter values, allows faster convergence employing few control parameters and provides a single model parameter vector which is imperative to this study.~~

These parameter vectors ~~model parameters~~ were estimated for each region assuming spatio-temporally constant/variable (wherever possible) parameter distribution. ~~sets. Depending upon the model variants, some parameters were distributed based on aspect and elevation.~~ The parameters were estimated within a plausible range as described in different snow modelling studies.

ROPE was applied to calibrate the snow-melt models, the HBV model with snow, and the modified HBV with external melt for this study. Nash-Sutcliffe Efficiency (NSE, Eq.(11)) ~~for overall, winter and snow days time-series~~ was used to evaluate the performance of the melt inputs, where the simulated and observed variables refer to modelled and observed discharge at time t.

$$NSE = 1 - \frac{\sum_{t=1}^{T} \left(Y_o^t - Y_m^t \right)^2}{\sum_{t=1}^{T} \left(Y_o^t - \bar{Y}_o^T \right)^2} \tag{11}$$

Where,

Y_m^t = Simulated variable at time t,

Y_o^t = Observed variable at time t,

$\bar{Y}_o^T$ = mean of observed variable for the time period T,

T = length of time series,

3.3 Model validation

The calibrated parameter vectors ~~sets~~ were used to validate the simulated snow-patterns for different seasons in the same year and as well as other years. The regional validation was done on several individual images representing unique events, as well as on sets of images representing different seasons for both BW and Switzerland. To analyse the performance of the snow models at a catchment level and subsequently for the discharge evaluation, five catchments viz. Neckar-Horb and Neckar-Rottweil in BW, and Reuss-Seedorf, Thur-Andelfingen and Aare-Brienzwiler in Switzerland, were selected. The radiation based melt model (Model 6) was calibrated for each catchment on daily snow-cover images with more than 60% valid pixels (< 40% cloud cover) for the winter season in different years. The winter season was selected as November - April (2010-2015) for BW and October - June (2010-2018) for Switzerland, assuming a reliable snow cover being present for the time period. To validate the performance of snow-cover based calibration on the snow-melt models, the HBV model was modified to accommodate the snow accumulation and melt of the calibrated snow models. The melt outputs from the calibrated snow models were fed into the modified HBV as standalone inputs. The modified HBV was then calibrated using ROPE on discharge for each catchment to evaluate the impact of the melt coming in as an input and to compare with a calibrated HBV model. ~~Once the model performance was adequately validated and the parameters were deemed 'applicable', the models were run again to obtain the gridded melt outputs, assuming the model predicted both the snow distribution as well as the water content adequately.~~

3.4 Model uncertainty

A common problem of hydrological modelling is that due to the inaccurate observations and simplified representation of the relevant hydrological processes, the parameters of the models cannot be identified accurately. Due to this equifinality, a set of acceptable model parameters can be assessed. If one can use specific additional information, the set of acceptable model parameters may reduce, leading to uncertainty reduction. In the case of snow modelling, the parameters of a hydrological model can be split into two distinct parts, the snow accumulation and melt parameters θ_s and the other model parameters θ_m. If the snow model parameters θ_s are calibrated independently of the model parameters, θ_m ~~one calibrates the snow model parameters θ_s independently of the model parameters~~, one receives a parameter set M_s - as the same problem of equifinality occurs for the snow models too. For each $\theta_s \in M_s$, one can calibrate the hydrological model parameters θ_m leading to a set M_m. This way ~~one obtains~~ a well performing parameter set $M_{sm} = M_s \times M_m$ can be obtained. However if ~~one can calibrate~~ the parameters of the model θ_m can be calibrated such that the model quality is the same as for calibrating the parameters (θ_s, θ_m) jointly (without using snow observations) obtaining the parameter set M, then the parameter set $M_{sm} = M_s \times M_m \subset M$. This is because all parameter combinations in M_{sm} could also be obtained from the traditional model calibration, but there are parameters in M where parameter compensations lead to snow parameters θ_s which are not acceptable for the snow model evaluation. Thus model calibration of conceptual model may not ~~cannot~~ lead to a better model performance, but instead can reduce uncertainty. On the other hand, the separate calibration of the hydrological model and the snow-melt model makes it possible to include more parameters into the snow model. If the same model would be calibrated together with the hydroligcal model, the increase of the number of parameters would lead to a much more complex calibration procedure. In the results section this is demonstrated for the models considered.

4 Results

Kriging performance across all the stations for both regions. The results suggest that the adopted Kriging procedure adequately mimics the daily precipitation from the stations in both regions. The NSEs range from 0.56 to 0.97 for the time period between 2010 and 2018 in Switzerland whereas for Baden-Württemberg the values ranged from 0.72 to 0.97. The station locations along with the corresponding NSE performance in the Swiss region is shown in Figs. 5a and 5b below. The figures show that the NSE performance for the winter precipitation decreases with increasing elevation. This loss in performance can be attributed to less density of stations in the higher elevation. However, the NSE values of greater than 0.6 for all but one station indicate that the Kriging process works satisfactorily in the region. The precipitation Kriging in Baden-Württemberg, however, did not depict a topographical trend in NSE performance, but the results highlight the applicability of the Kriging in the region. It can also be observed from Table 3 that the EKD Kriging was very much efficient in interpolating mean temperature in both the regions.
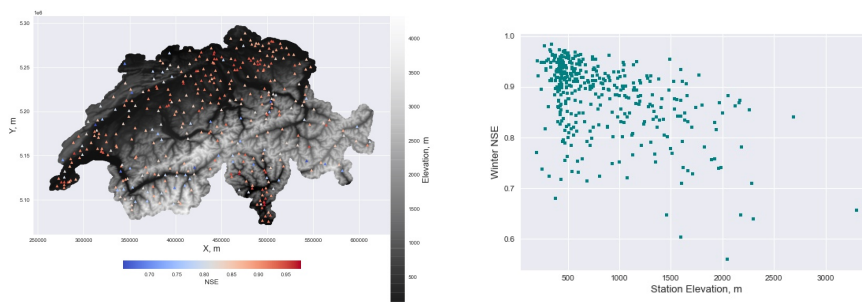
(a) NSE in different precipitation stations

(b) NSE performance of Kriged precipitation at different station elevation

Figure 5. Kriging performance in terms of NSE in Switzerland

4.1 Model Results

Switzerland

For Switzerland, a relatively cloud-free MODIS image for 18th January 2012 was selected as a reference day with snow, and all the model variants were calibrated on~~using~~ this reference image. All of the six models reported good Brier-scores. The normalized confusion statistics~~matrices~~ calculated for the reference day with all models along with their Brier-scores are shown in Table 4 ~~Fig.6a~~. The columns of the confusion statistics table~~top-left, top-right, bottom-right and bottom-left boxes of a confusion matrix plots~~ respectively indicate the proportions of true negatives (both 'no snow'), false positives (MODIS: 'no snow', simulated: 'snow'), true positives (both 'snow') and false negatives (MODIS: 'snow', simulated: 'no snow'). Table 4 shows gradual improvement in the model performance with additional parameters, with the Brier-scores ranging from 0.044 to 0.0365. Model 6 including the radiation induced snow-melt shows the best performance among the models, with a Brier-score value of 0.0365. Model 5 has the next closest match. The models 5 and 6 both improve the true negatives and true positives

Table 3. Summary of mean Kriging performance in the study regions

Region	Variables	Reference period	Pearson correlation	Rank correlation	RMSE	NSE	No. of stations
Switzerland	Mean temp.	Overall	0.99	0.99	1.13	0.971	365
		Winter	0.978	0.977	1.288	0.936	
	Precipitation	Overall	0.933	0.83	2.637	0.856	449
		Winter	0.95	0.823	2.166	0.883	
Baden-Württemberg	Mean temp.	Overall	0.992	0.992	0.938	0.978	85
		Winter	0.979	0.976	0.982	0.943	
	Precipitation	Overall	0.907	0.876	2.295	0.811	128
		Winter	0.96	0.912	1.479	0.901	

with Model 6 exhibiting lesser false recognition of snow. With a more balanced representation of false and true positives and negatives, Model 6 was selected as the best model and is thus used as the reference model for further analysis. Figure 7a shows the simulated snow image for the reference day using the best model along with the differences from MODIS. The left plot in the figure is the MODIS image for the reference day, the central plot shows the simulated image for the day and the right one shows the differences in prediction.

Table 4. Normalized confusion matrices for 2012-01-18 calibration in Switzerland

	True Positive	False Positive	True Negative	False Negative	Brier-scores
Model 1	0.954	0.046	0.962	0.038	0.0422
Model 2	0.96	0.04	0.958	0.042	0.0409
Model 3	0.975	0.025	0.935	0.065	0.0441
Model 4	0.975	0.025	0.947	0.053	0.0381
Model 5	0.968	0.032	0.957	0.043	0.0373
Model 6	0.975	0.04	0.956	0.044	**0.0365**

Figure 8a below shows the normalized confusion matrix of MODIS snow-cover and snow-cover simulated by the best model (driven by the parameters calibrated for the aforementioned reference day), for a period of 2011-01-01 to 2018-12-31. The matrix reflects very good capability of the model to identify and predict snow ('1') with 0.947 and no-snow pixels ('0') with 0.932 as a proportion of all the valid pixels. The false negatives and true negatives amount to less than 10 % of the total pixels.

(a) Normalized Confusion matrices from all models for the reference day (‚1‘: Snow, ‚0‘: No snow)
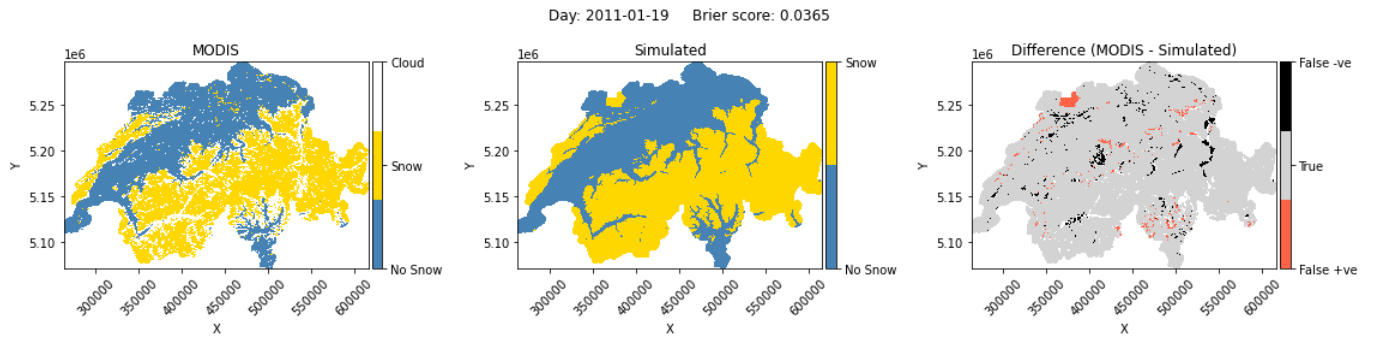
(b) MODIS inferred snow distribution (left) vs Model 6 simulated distribution (centre) and differences between MODIS and simulated (right)

Figure 6. Simulation results for the reference day of 2012-01-18 for Switzerland

Day: 2011-01-19   Brier score: 0.0365

(a) Switzerland

Day: 2010-02-27   Brier score: 0.1056
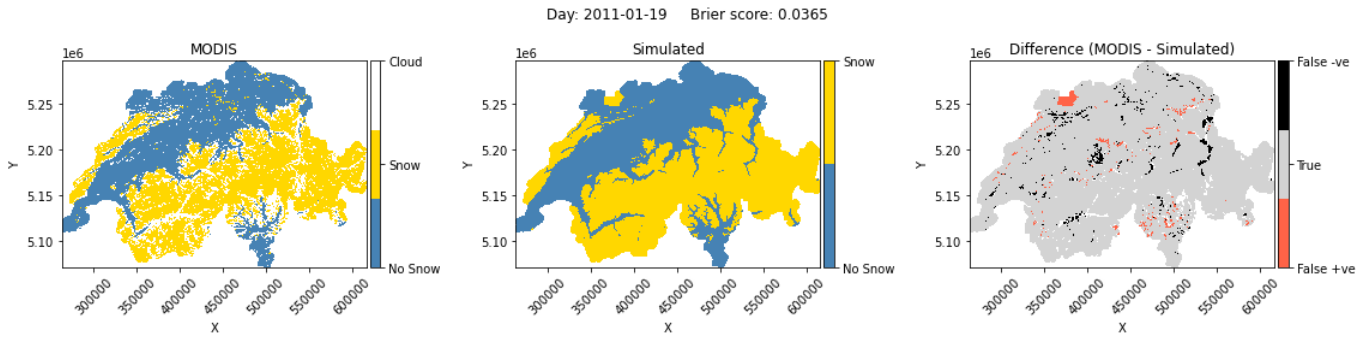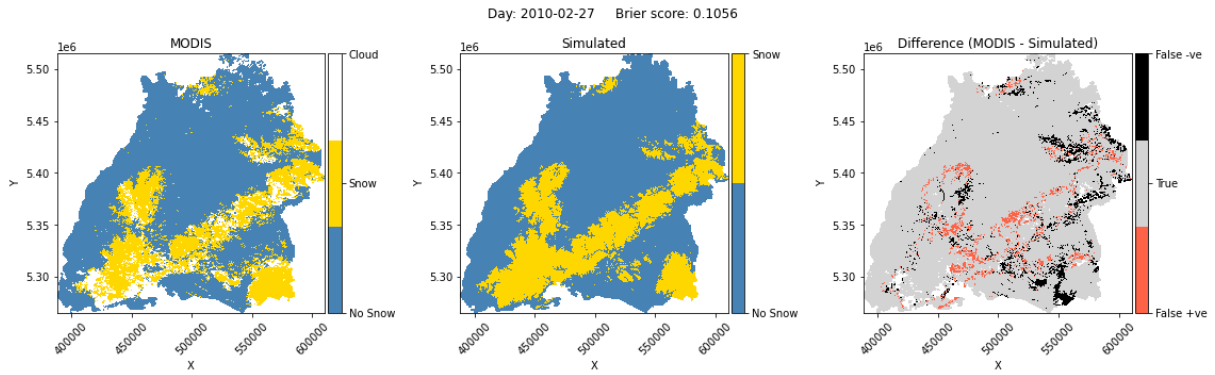
(b) Baden-Württemberg

Figure 7. Regional Simulation results for the reference days - MODIS inferred snow distribution (left) vs Model 6 simulated distribution (centre) and differences between MODIS and simulated (right)
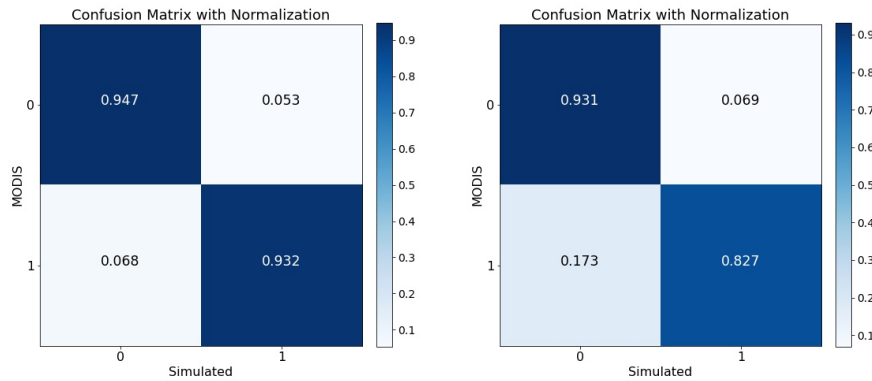
(a) Switzerland   (b) Baden-Württemberg

Figure 8. Normalized confusion matrices of the simulation results for 2011-2018 in Switzerland and 2011-2015 in BW

Baden-Württemberg

The different snow models were also tested in BW region in Germany. The region was selected to test the efficacy of the approach in shorter duration snow region. MODIS image for the day 2010-02-27 was selected as the reference image for calibration. As in Switzerland, all models were able to mimic the snow-distribution pattern for the reference day well where Model 6 performed the best in terms of the Brier-score and is shown in Fig. 7b. The models were further validated for different cloud free days in different years as well.

The simulations were able to capture the snow-distribution reasonably well in BW, albeit not as good as in Switzerland. Short duration snow or lesser snow availability can be attributed to this drop in model performance, as it imparts added uncertainty in model prediction. Based on the Brier-scores on the validation days, Model 6 was selected as the reference model and from hereon used for further analysis based on the validation data. Figure 8b shows the normalized confusion matrix based on Model 6 simulation from 2011-01-01 till 2015-12-31 using the images during the time-period. It is evident from the figure that the model is able to simulate the snow-distribution well enough with 83 % of correctly identified 'snow' pixels. This performance, however, shows that the model still has room for improvement especially in regions like BW, where snow-melt has a major implication on water availability is a major source of water.

4.2 Transferability of model parameters

To test for the transferability of the model parameters through different seasons, the calibrated model parameters were also validated on the set of available snow cover images for the average onset and average melting seasons of different years. The goal here, was to investigate a relatively stable parameter-set across the time domain that can depict comparable model performance for different seasons. A Results from a calibrated well-performing parameter vector was used to compare the results in different seasons. The best model (Model 6) is used as the reference model in this analysis. Snow onset periods (Oct-Dec for Switzerland and Nov-Dec for BW) and melting periods (Jan-Mar for Switzerland and Jan-Feb for BW) for 2010 - 2015 were selected as the calibration and validation periods. The models were calibrated for onset periods for each year and then run to forecast the snow distribution in the corresponding melting season as well as to hindcast the snow distribution in the onset and melting seasons of preceeding year. Tables 5 and 6 below summarize the model performance (Brier-score) for different simulation hindcast and forecast periods for Switzerland and BW, respectively. The '*', '**' and '***' highlights depict hindcast, calibration and forecast for each year.

For example As an illustration, in Switzerland, the model was calibrated for 2011 Oct-Dec period and used to hindcast the snow cover distribution in the preceding onset (2010 Oct-Dec) and melt (2011 Jan-Mar) seasons, and forecast for the corresponding melting season (2012 Jan-Mar). The 2011 model performance was then compared with the hindcast of the succeeding calibration and the forecast of the previous calibration. Here in this example the hindcast performance (0.068 for Oct-Dec 2010 and 0.0661 for Jan-Mar 2011) is very close to the ones simulated by the 2010 model (0.0675 for calibration period and 0.061 for forecast period). The other results are also comparable throughout the years. These results are again compared with the model calibrated on a single day image in the last column (2012-01-18) described in earlier sections. Here

Table 5. Model calibration, hindcast and forecast performance in different seasons for Switzerland

Validation Periods	Calibration Periods						
	2010/ Oct-Dec	2011/ Oct-Dec	2012/ Oct-Dec	2013/ Oct-Dec	2014/ Oct-Dec	2015/ Oct-Dec	Jan 18 2012
2010/ Jan-Mar	0.0683*						
2010/ Oct-Dec	0.0676**	0.0685*					0.0734*
2011/ Jan-Mar	0.0607***	0.0661*					
2011/ Oct-Dec		0.0853**	0.0862*				0.0906*
2012/ Jan-Mar		0.0512***	0.0597*				
2012/ Oct-Dec			0.0803**	0.0855*			0.0886**
2013/ Jan-Mar			0.0665***	0.0567*			
2013/ Oct-Dec				0.1005**	0.1244*		0.1064***
2014/ Jan-Mar				0.0510***	0.0631*		
2014/ Oct-Dec					0.0728**	0.0748*	0.0894***
2015/ Jan-Mar					0.0999***	0.0827*	
2015/ Oct-Dec						0.0910**	0.0975***
2016/ Jan-Mar						0.0937***	
							* Hindcast ** Calibration *** Forecast

Table 6. Model calibration, hindcast and forecast performance in different seasons for BW

Validation Periods	Calibration Periods							Swiss parameters for 01.12.2018
	2010/ Nov-Dec	2011/ Nov-Dec	2012/ Nov-Dec	2013/ Nov-Dec	2014/ Nov-Dec	2015/ Nov-Dec	Feb27 2010	
2010/ Jan-Feb	0.119*						0.115**	
2010/ Nov-Dec	0.078**	0.085*					0.085***	**0.083***
2011/ Jan-Feb	0.179***	0.231*						
2011/ Nov-Dec		0.240**	0.238*				0.255***	**0.255***
2012/ Jan-Feb		0.298***	0.281*					
2012/ Nov-Dec			0.234**	0.237*			0.241***	**0.24***
2013/ Jan-Feb			0.215***	0.179*				
2013/ Nov-Dec				0.296**	0.373*		0.324***	**0.324***
2014/ Jan-Feb				0.218***	0.306*			
2014/ Nov-Dec					0.228**	0.234*	0.236***	**0.236***
2015/ Jan-Feb					0.245***	0.251*		
2015/ Nov-Dec						0.205**	0.209***	
								* Hindcast ** Calibration *** Forecast

as well, the model calibrated on a single image is able to adeptly track the distribution in different snow-onset and melt seasons in different years, without much loss in performance.

480   As an~~For~~ illustration, a set of good parameter vector for the aforementioned seasons and the reference day are shown below in Figures 9a and 9b. The P_T and D_w parameters are less sensitive and the fluctuations in these parameters do not have major implications on the model performance. Apart from these parameters, it is apparent that the individual parameter values do not fluctuate a lot and are more or less stable in Switzerland. The calibrated parameters from the single day calibration, understandably shows quicker melt with low values of snow-melt temperatures, apart from which the parameter sets can be

485 inferred as temporally stable for the said periods for this region. However, individual parameter values here have a wider spread in BW for the same periods in comparison with Switzerland. As discussed above, this can be attributed more to the lesser and more uncertain availability snow in different seasons. This shows that with continuous updating of the approach~~model~~ for each season, the model has the potential to~~can~~ forecast the snow-availability.

(a) Switzerland

(b) Baden-Württemberg

Figure 9. Calibrated parameter sets for Oct-Dec periods in different years

4.3   Snow-melt model results at catchment level

As explained above, the snow-melt models were calibrated for two catchments in BW and three in Switzerland on snow-cover distribution with less than 40% cloudy pixels for the winter season throughout the entire reference period. ROPE was used to calibrate the models and obtain 1000 sets of best performing parameter vectors for each catchment, based on the overall Brier-scores. The simulated snow-cover distribution was compared with the ones estimated by the HBV's snow-routine to assess the representation of snow accumulation and melt processes within. The 1000 HBV snow parameter sets were subsetted from the best performing parameter vectors obtained during ROPE calibration of the HBV model on discharge for each catchment. The comparison results are shown in Fig.10 below. It is evident from the violin plots that the snow-melt models clearly out-perform the HBV snow routine in all catchments while estimating the snow-cover distribution estimation.The median Brier-score values for the snow-melt models in all catchments are lesser than their counterparts. Moreover, the 1000 best Brier-score values for the snow-melt models depict a very narrow spread in contrast to a much wider spread from the HBV's snow routine. This shows the uncertainty of the HBV during the simulation of snow accumulation and melt, which hints towards a compensating effect with other non-snow parameters. This spread is more pronounced in the Horb and Rottweil catchments, which are characterized by shorter duration snow. The results suggest that HBV's snow routine, when calibrated on discharge together with the other model parameters, is not able to capture the snow dynamics in BW region as compared to the spread in Swiss catchments with longer duration snow. This approach thus adds value to these regions as the calibrated snow cover distribution provide a strong basis for estimating available water coming from snow, as these regions are dependent of ~~on~~ the melt waters. The results, thus strongly indicate that the use of a standalone snow-melt model, in this study, provides a very stable and reliable representation of the snow-cover distribution and in turn the melt.

The boxplots showing the dispersion of the parameters are shown below in Fig.11. The y axis shows the normalized parameter values based on their min-max range set for optimization. The boxplots indicate that apart from the radiation melt factor, r_{ind}, T_{Mmax}, T_{Mmin} and to some extent T_S, all the parameter ranges are relatively stable and less sensitive to the model performance. These four parameters are however constrained by the objective function and it is understandably so because these parameters are more sensitive as they govern the appearance and disappearance of the snow.

4.4 Validation in hydroligcal models~~Hydrological Models~~

The best performing parameter vector from the snow-melt models for each catchment was used to simulate the melt waters exiting the snow-regime, which was in turn, used in the modified HBV model to simulate the hydrologic implications of the melt as a standalone input. The modified HBV was calibrated on discharge for the whole timeseries for each of the catchments. This was done with 3 iterations of ROPE. The standard HBV was also calibrated on the same discharge data, but with five ROPE iterations. With the ROPE calibration, 1000 robust parameter sets were identified for both hydrological models. The best NSEs were subsequently compared to assess the performance of the snow-melt models against the HBV. The results are shown below in Fig.12 and Table 7.

The results show that the addition of melt significantly improves the hydrological model performance in each of the catchments, notably the most in the snow dominated ones in Reuss and Aare. The median NSEs show improvement in all of the catchments in the study domain. The NSE spread is also smaller in the modified HBV. This highlights uncertainty reduction, as
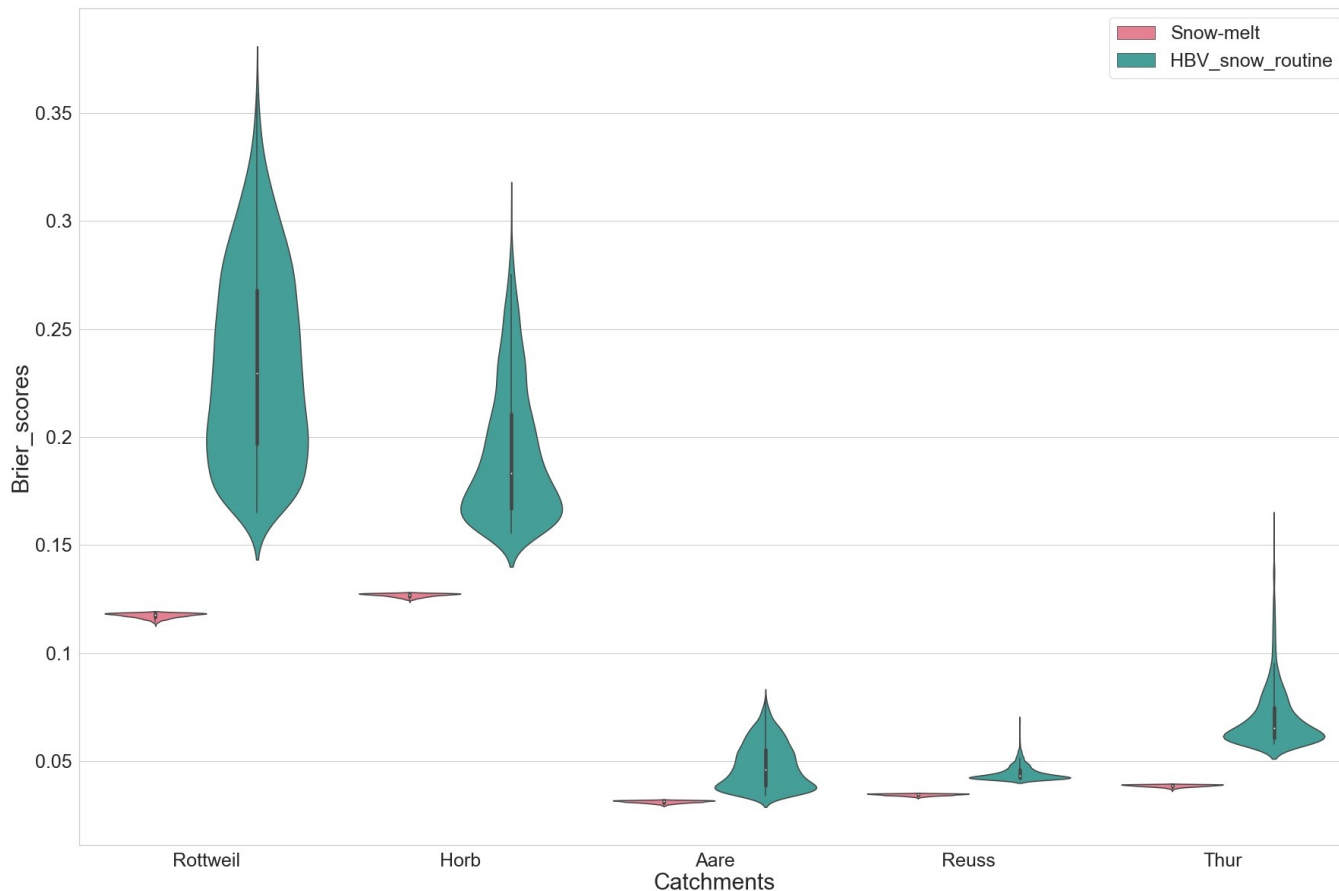
Figure 10. Violin plots comparing the performance of snow-melt models and HBV's snow routine in terms of Brier-scores

the hull containing the equifinal parameter vectors becomes smaller as a result of lesser parameters to calibrate for the modified HBV variant. The results suggest that the improvement in model performance comes with a better computational efficiency and a better 'mimicry' of the snow accumulation and melt.

Furthermore figures 13a and 13b show an illustration of an isolated hydrological simulation in Horb catchment for the winter of 2012-13. The figures show that the melt input adds value to the discharge simulation during the season quite efficiently as compared to its HBV counterpart. The 1000 best hydrographs envelope the observed discharge better than the HBV model indicating a better representation of the snow-melt process.

~~Once the simulated snow cover distribution from the melt models were validated for cloud free days in the respective regions, the melt outputs from the models were used as standalone inputs to a modified HBV („the Liquid HBV") and the resulting flows compared with the basic HBV model for the entire, winter and snow-days time-series. This was done for Neckar and Horb catchments in Baden-Württemberg and Reuss catchment in Switzerland. Horb, a tributary of the Neckar catchment, was selected as the catchment is predominantly snow-fed and shows direct response to snow-melt. The basic HBV model was first~~
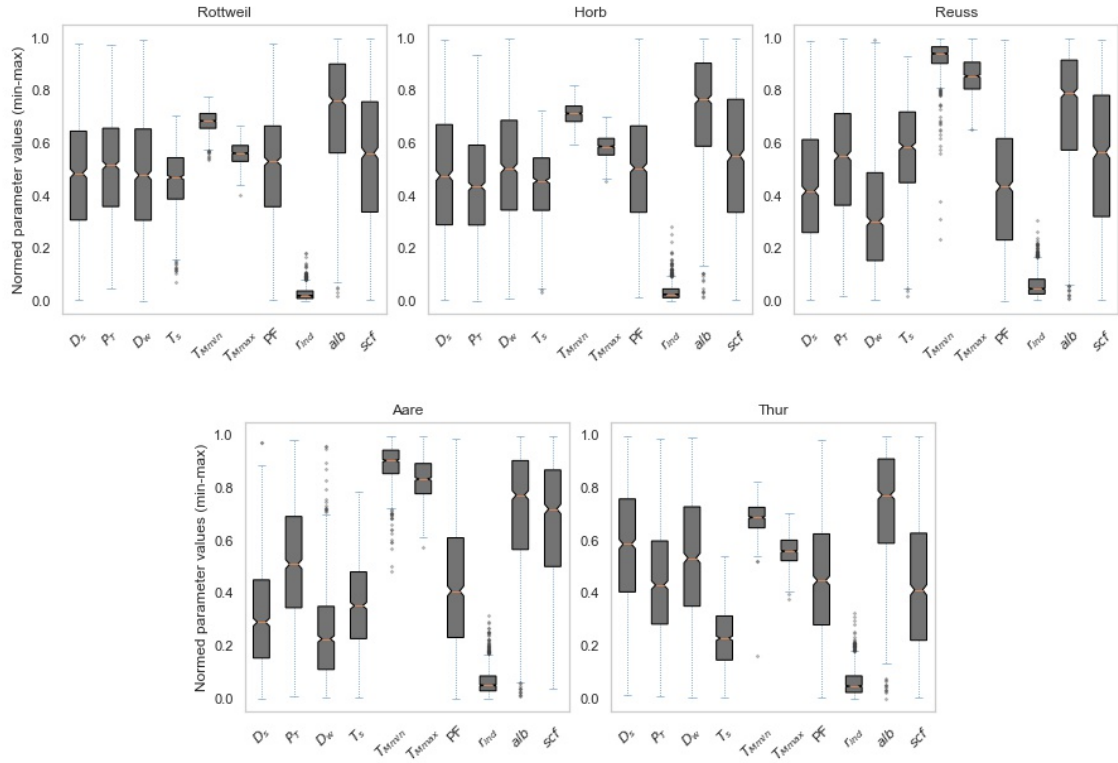
Figure 11. Snow-melt model parameter dispersion

Table 7. Comparison of HBV and Modified HBV NSE performance

	HBV NSEs			Modified HBV NSEs		
	Min	Max	Median	Min	Max	Median
Rottweil	0.595	0.672	0.609	0.663	0.724	0.676
Horb	0.653	0.700	0.663	0.738	0.821	0.755
Aare	0.395	0.566	0.424	0.658	0.678	0.663
Reuss	0.635	0.779	0.656	0.781	0.796	0.785
Thur	0.702	0.768	0.712	0.731	0.776	0.739
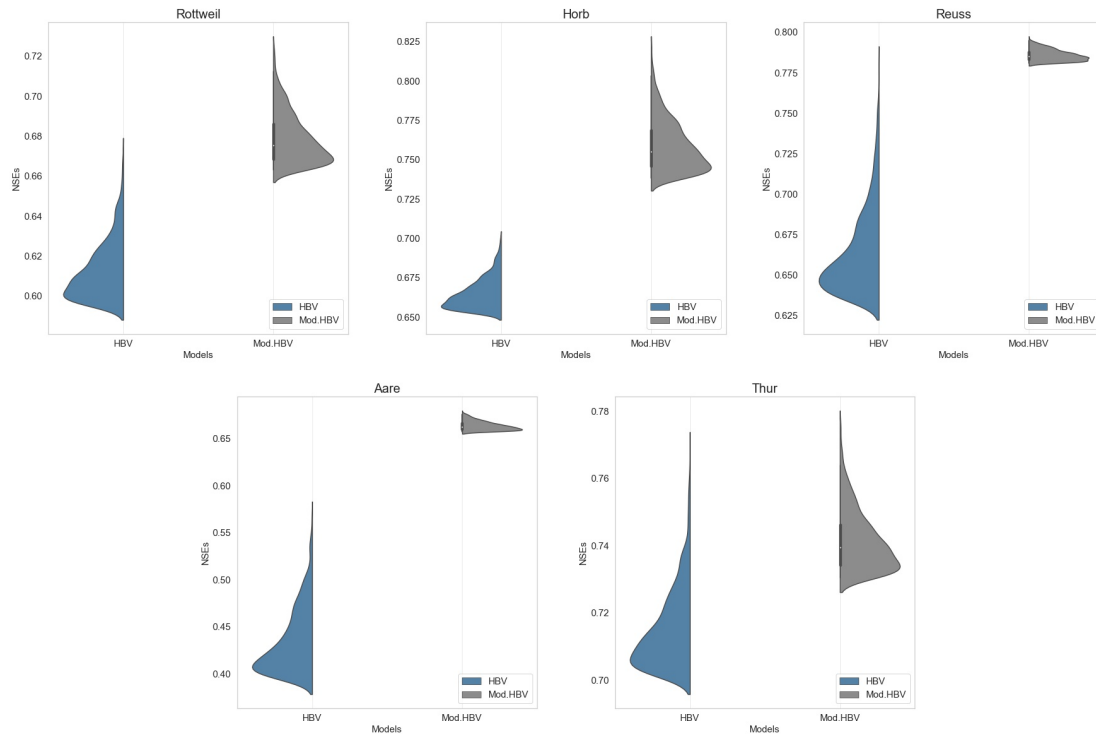
Figure 12. Performance comparison of the hydrological models in terms of NSE

calibrated for each of the catchments and the calibrated parameters (without the snow parameters) were used in the liquid HBV model and the flows were compared. The performance of different model outputs in HBV respectively for Neckar and Horb is shown below in Tables 8a and 8b. Likewise, the hydrographs from the best models are shown below in Figs. 14a-14d.Similarly, this validation was also done in Reuss catchment in Switzerland. The results are shown below in Table 10 and Figs.16a and 16b.

540 The results and the hydrograph plots show increased overall as well as winter performance in terms of NSE in almost all the catchments. The improvement in NSEs, albeit less, is notable. This can be further explained by the reduction in mean squared errors by 15% in Reuss, 11.5% in Neckar and 3.8% in Horb. It can be thus be argued that the snow-distribution calibrated models can bolster the hydrological model outputs with an added reliability of snow-distribution.

Table 8. Performance evaluation of the snow-model outputs in HBV

(a) Neckar in Baden-Württemberg

Models	Overall NSE	NSE, winter	NSE, Snow days	Model description
Basic HBV	0.871	0.858	0.841	HBV with snow component
Liq HBV + Model 1	0.869	0.853	0.834	Standard DDF melt
Liq HBV + Model 2	0.876	0.867	0.853	Model 1 + precipitation induced melt
Liq HBV + Model 3	0.867	0.854	0.834	Model 2 + sftmp + smtmp
Liq HBV + Model 4	0.868	0.855	0.825	Model 2 + smtmp + distributed sftmp
Liq HBV + Model 5	**0.885**	**0.881**	**0.872**	Model 2 + sftmp + distributed smtmp
Liq HBV + Model 6	0.871	0.86	0.841	Model 3 + Radiation induced melt
Liq HBV + Model 6.1	0.874	0.864	0.848	Model 5 + Radiation induced melt

(b) Horb in Baden-Württemberg

Models	Overall NSE	NSE, winter	NSE, Snow days	Model description
Basic HBV	0.841	0.844	0.807	HBV with snow component
Liq HBV + Model 1	0.793	0.779	0.7	Standard DDF melt
Liq HBV + Model 2	0.834	0.835	0.788	Model 1 + precipitation induced melt
Liq HBV + Model 3	0.846	0.85	0.811	Model 2 + sftmp + smtmp
Liq HBV + Model 4	0.845	0.848	0.809	Model 2 + smtmp + distributed sftmp
Liq HBV + Model 5	0.846	0.85	0.811	Model 2 + sftmp + distributed smtmp
Liq HBV + Model 6	**0.847**	**0.851**	**0.813**	Model 3 + Radiation induced melt

Table 9. Performance evaluation of the snow-model outputs in HBV for Reuss catchment in Switzerland

Models	Overall NSE	NSE, winter	NSE, Snow days	Model description
Basic HBV	0.859	0.833	0.859	HBV with snow component
Liq HBV + Model 1	0.861	0.834	0.861	Standard DDF melt
Liq HBV + Model 2	0.865	0.841	0.865	Model 1 + precipitation induced melt
Liq HBV + Model 3	0.876	0.856	0.876	Model 2 + sftmp + smtmp
Liq HBV + Model 4	0.87	0.848	0.87	Model 2 + smtmp + distributed sftmp
Liq HBV + Model 5	**0.878**	**0.858**	**0.878**	Model 2 + sftmp + distributed smtmp
Liq HBV + Model 6	**0.873**	**0.853**	**0.88**	Model 3 + Radiation induced melt

(a) HBV model
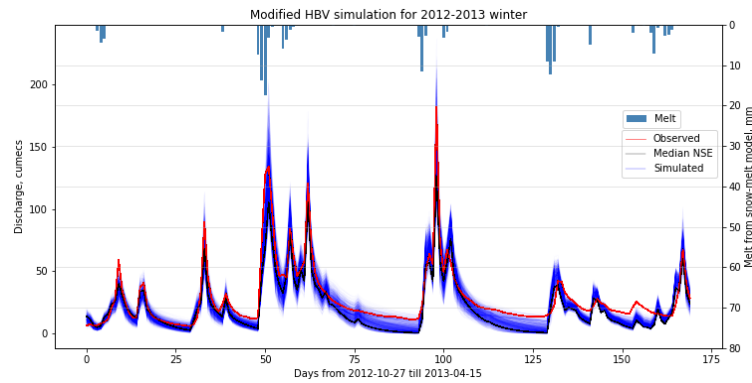
(b) Modified HBV model

Figure 13. Simulated hydrographs for the 2012-13 winter

Table 10. Performance evaluation of the snow-model outputs in HBV for Reuss catchment in Switzerland

Models	Overall NSE	NSE, winter	NSE, Snow days	Model description
Basic HBV	0.859	0.833	0.859	HBV with snow component
Liq HBV + Model 1	0.861	0.834	0.861	Standard DDF melt
Liq HBV + Model 2	0.865	0.841	0.865	Model 1 + precipitation induced melt
Liq HBV + Model 3	0.876	0.856	0.876	Model 2 + sftmp + smtmp
Liq HBV + Model 4	0.87	0.848	0.87	Model 2 + smtmp + distributed sftmp
Liq HBV + Model 5	**0.878**	**0.858**	**0.878**	Model 2 + sftmp + distributed smtmp
Liq HBV + Model 6	**0.873**	**0.853**	**0.88**	Model 3 + Radiation induced melt

(a) Standard HBV   (b) Modified HBV with melt from Model 5

(c) Standard HBV   (d) Modified HBV with melt from Model 6

Figure 14. ~~Simulated and observed hydrographs with NSE performance in Neckar in Baden-Württemberg (upper row: Neckar catchment, lower row: Horb catchment)~~

(a) Standard HBV   (b) Modified HBV with melt from Model 5
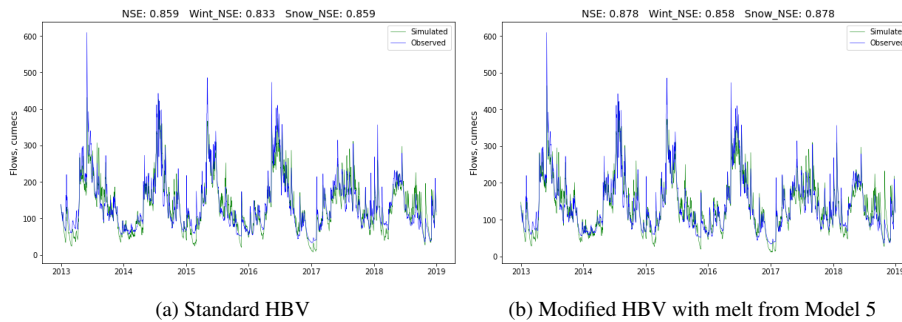
Figure 15. ~~Simulated and observed hydrographs with NSE performance in Reuss catchment, Switzerland~~

5   Discussion

545   It is a big challenge and a highly imperative one, to improve the snow-melt routines in widely and successfully tested rainfall-runoff models like HBV (Bergström, 2006; Girons Lopez et al., 2020). With this backdrop, this study implemented a new image-based pattern calibration approach using MODIS-inferred snow- cover distribution for a number of cloud free days ~~certain cloud-free day and for a duration of snow season of a given year.~~ The MODIS data available freely across the world

(a) Standard HBV   (b) Modified HBV with melt from Model 5
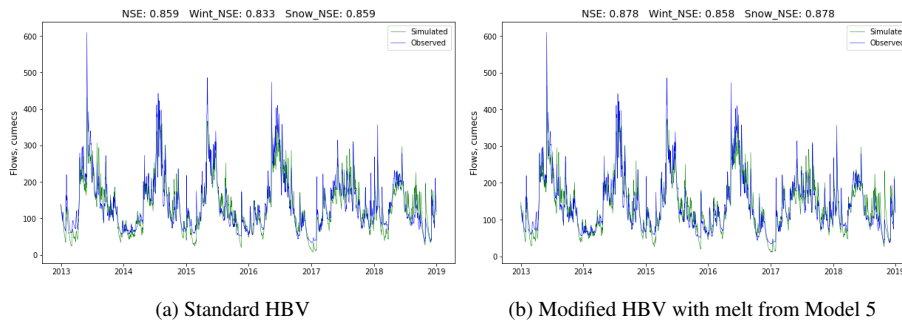
Figure 16. ~~Simulated and observed hydrographs with NSE performance in Reuss catchment, Switzerland~~

and at a daily resolution, provides a plausible alternative to ground based data for immediate verification of snow-melt models.
550 Widely used and computationally simplistic temperature index models with low data requirement were considered in the study and were modified wherever possible, to gain enhanced model performance.

~~The Residual Kriging incorporating X,Y coordinates and directionally smoothed DEMs showed very good agreement in Switzerland and Baden-Württemberg regions during the leave-one-out cross validation for the winter season .(October – April) ranging from For temperature, the External Drift Kriging was also able to simulate the observed values in both regions.~~ We found~~further~~
555 ~~found out~~ that all the model variants calibrated on a set of individual snow-cover images were able to track the MODIS snow-distribution with good~~higher~~ accuracy. T~~However, t~~he melt-model with daily potential clear-sky radiation, for both regions was able to ~~perform the best among the considered model variants in both regions. The model was able to~~ simulate the snow cover distribution with a higher accuracy in identifying~~to identify~~ snow and no-snow pixels, reflected on the low Brier-score values. ~~The calibrated model was also able to track the evolution and depletion of snow adeptly throughout the snow seasons~~
560 ~~in different years.~~ The inclusion of radiation induced melt provides a more realistic spatial distribution of melt rates (Hock, 1999). To assess the temporal stability across different seasons in different years, a set of well-performing parameter vector calibrated on sets of multiple snow-cover images for different seasons using the radiation-based melt model, were chosen.~~The model parameters were then tested for temporal stability across different seasons and years.~~ The hindcasting, calibration and forecasting results show that model parameters calibrated for each season are more or less stable without much fluctuations, in
565 Switzerland. This was, however, slightly different in Baden-Württemberg as the calibrated parameters for different years depicted higher scatter. This could be due to lesser and more uncertain snow-availability in comparison to Switzerland. It is to be noted that the parameters identified as optimum for the Swiss regions also perform well for Baden-Württemberg~~as compared to the calibrated Brier-scores in all the calibration periods~~. This highlights the potential of the approach~~bolsters the objective of this study~~ to obtain spatio-temporal robustness of the model parameters. ~~We found out that with continuous model updating,~~
570 ~~the data can be used to guide the snow-melt forecast in the regions with snow-melt as primary water source.~~

On a catchment level, three catchments in Switzerland and two in BW were selected. The snow-melt model was calibrated using multiple images for winter seasons throughout the time period to obtain a set of 1000 robust parameter vectors. The temperatures demarcating snow and melt onset and the radiation melt factor were deemed sensitive to the overall Brier-scores.

The Brier-scores from these 1000 simulations were compared with the ones estimated with parameters in the HBV's snow routine. The calibrated snow model significantly outperforms the HBV's snow model calibrated on discharge in all of the catchments. This has also been discussed by Udnæs et al. (2007) and Parajka and Blöschl (2008) in their respective studies that calibration on SCA in addition to runoffs improved the snow model efficiency. Further, our results clearly show that the uncertainty in simulation of the snow-cover distribution is significantly reduced when using a dedicated snow-melt model, as the snow parameters in the HBV calibrated on discharge are compensated with other non-snow parameters. This compensation leads to a more uncertain representation of the snow accumulation and melt dynamics. This decrease in uncertainty with a simplified calibration approach using freely available data is noteworthy as the calibrated parameter vectors are more robust as compared to the ones calibrated on discharge. Similar findings have been pointed out by Riboust et al. (2019) where they discussed the increased robustness of the snow model parameters when SCA was added into the calibration.

To further test the implication of the melt outputs from the snow models, the melt estimated with the best performing snow-model parameter vector, was used as a standalone input to a HBV model modified to accommodate the external melt information in all the five catchments. The HBV and its modified variant were calibrated on discharge separately, thereby estimating 1000 robust parameter sets. The results suggest improvement in the NSE performance in all the catchments while using the modified HBV. Parajka and Blöschl (2008) also concluded that the median runoff model efficiency increased when MODIS data was used for the calibration in comparison to a traditional dicharge calibration. Bennett et al. (2019) also concluded in a similar tune with their results showing MODIS fSCA improving the internal snow timings as well as the hydrological simulations.

Our results further show that the NSE dispersion is also reduced with the modified HBV simulations indicating a reduction in model uncertainty as the set of equifinal parameters becomes smaller. This gain in performance comes with better computational efficiency, as the modified HBV calibration converges faster. The use of the more complex snow models in HBV, without calibrating them on snow cover observations is difficult as the number of parameters increases. However, with a dedicated snow-melt model, this can be achieved as it is relatively quicker to calibrate on the images and the resulting melt can be used in the hydrological models for efficient calibration. Di Marco et al. (2021) also concluded that a combination of MODIS fractional snow cover area and streamflow data led to a reduction of predictive uncertainty of a hydrological model thereby leading to sharper and reliable flow simulations. Furthermore, the strength of this approach lies in the simplicity, spatial flexibility and global availability of the model input data which can be very useful for data scarce regions. ~~Finally, the melt outputs from the best models were selected as standalone inputs to a modified HBV model and the resulting hydrographs for Reuss in Switzerland and, Neckar and Horb in Baden-Württemberg were assessed. The results suggested that these modified HBV model had slightly better NSE performance than the calibrated HBV models for the catchments in the region. However, 3.8-15% decrease in mean squared errors were observed for all the catchments under study. The not-so-significant gain in NSE performance can be attributed to HBV's simplistic generalization of the real processes and the behaviour outputs at the chosen spatio-temporal resolution . Nevertheless, we were able to infer that the improvement in NSEs, albeit less, can be achieved with an added reliability of snow-distribution.~~

6 Conclusions

We assessed the potential of freely available snow cover distribution from daily resolution MODIS data to calibrate the snow-melt models on snow-pattern instead of a more traditional SWE and flow based calibration in the snow-dominated regimes in Switzerland and Baden-Württemberg region in Germany. Specifically, different model modifications were employed to assess the improvement in the simulation of snow-distribution with lesser input requirements. It was observed that the methodology does well in mimicking~~reproducing~~ the snow cover distribution in the regions with relative higher accuracy. Furthermore, comparison of the snow model's performance with the HBV's snow routine shows that the uncertainty in the representation of snow-accumulation and melt processes can be reduced with a standalone calibration of a snow-melt model as HBV calibration on discharge usually exhibit compensating behaviour with other non-snow parameters. This allows for incorporation of additional parameters in the independent snow-melt models to better represent the snow dynamics, as opposed to the fact that additional parameters in hydrological models impose further complexity during calibration. The assimilation of the independent melt from the snow-model outputs in a hydrological model further reduces the uncertainty related to hydrological simulation as the set of parameters required for calibration becomes smaller. This reduction in uncertainty was accompanied by improvement in model performance and a gain in computational efficiency with faster convergence. The improvement in model performance can be deemed for 'a right reason' with a better representation of the underlying snow processes. This highlights our finding that the simpler specific alterations to processes related to snow-melt can contribute to better simulation of the snow-distribution and the resulting flows in snow-dominated regimes.~~The application of the melt-model outputs in HBV increased the NSE performance to some extent and in conjunction with this approach, simpler specific alterations to processes contributing to snow-melt can contribute to identifying the snow-distribution and to some extent the flows in snow-dominated regimes.~~ We can thus, conclude that calibration using readily available images used in this method offers adequate flexibility, albeit the simplicity, to calibrate snow distribution in mountainous areas across a wide geographical extent with reasonably accurate precipitation and temperature data, especially in data scarce regions. The other data used for the snow models can be derived from publicly available digital elevation models. The reduction in model uncertainties, primarily with the snow-distribution estimation and with the discharge simulation, adds value to provide improved conceptualization of the temperature-index model routines and further potential model updating. Furthermore, this approach is not dependent on the choice of hydrological models as it can be extended to any hydrological model that can identify the snow-cover distribution.

Data availability. The precipitation and temperature data were obtained from the Climate Data Center of the German Weather Service (DWD; https://opendata.dwd.de/climate_environment/CDC, last access: 15 February 2021) (DWD, 2021) and the Swiss Federal Office of Meteorology and Clima-tology (MeteoSwiss; https://gate.meteoswiss.ch/idaweb, last access: 21 Decemeber, 2020)(MeteoSwiss, 2020). The MODIS snow cover images were downloaded using the Earth Data Search tool (https://search.earthdata.nasa.gov, last access: 19 Feb 2021). The DEM was obtained from http://srtm.csi.cgiar.org.

Author contributions. This study is a part of DG's doctoral research supervised by AB. The study was conceptualized by AB and DG, and was implemented by DG. Both authors contributed to the writing, reviewing and editing of the paper.

Competing interests. The authors declare that they have no conflict of interest.

Acknowledgements. The authors would like to acknowledge Deutscher Akademischer Austauschdienst (DAAD) for the doctoral research scholarship which encompasses this study.

Financial support. This open-access publication was funded by the University of Stuttgart.

References

Bárdossy, A. and Pegram, G.: Interpolation of precipitation under topographic influence at different time scales, Water Resources Research, 49, 4545–4565, https://doi.org/https://doi.org/10.1002/wrcr.20307, 2013.

Bárdossy, A. and Singh, S. K.: Robust estimation of hydrological model parameters, Hydrology and Earth System Sciences, 12, 1273–1283, https://doi.org/10.5194/hess-12-1273-2008, 2008.

Bárdossy, A., Anwar, F., and Seidel, J.: Hydrological Modelling in Data Sparse Environment: Inverse Modelling of a Historical Flood Event, Water, 12, https://doi.org/10.3390/w12113242, 2020.

Bennett, K. E., Cherry, J. E., Balk, B., and Lindsey, S.: Using MODIS estimates of fractional snow cover area to improve streamflow forecasts in interior Alaska, Hydrology and Earth System Sciences, 23, 2439–2459, https://doi.org/10.5194/hess-23-2439-2019, 2019.

Bergström, S.: Experience from applications of the HBV hydrological model from the perspective of prediction in ungauged basins, IAHS-AISH publication, pp. 97–107, 2006.

Bergström, S.: The HBV model., chap. Computer models of watershed hydrology, pp. 443–476, Water Resources Publications, Colorado, USA, 1995.

Beven, K.: How far can we go in distributed hydrological modelling?, Hydrology and Earth System Sciences, 5, 1–12, https://doi.org/10.5194/hess-5-1-2001, 2001.

Caicedo, D. R., Torres, J. M. C., and Cure, J. R.: Comparison of eight degree-days estimation methods in four agroecological regions in Colombia, Bragantia, 71, 299–307, https://doi.org/https://doi.org/10.1590/S0006-87052012005000011R, 2012.

Debele, B., Srinivasan, R., and Gosain, A.: Comparison of Process-Based and Temperature-Index Snowmelt Modeling in SWAT, Water Resources Management, 24, 1065–1088, https://doi.org/10.1007/s11269-009-9486-2, 2009.

Di Marco, N., Avesani, D., Righetti, M., Zaramella, M., Majone, B., and Borga, M.: Reducing hydrological modelling uncertainty by using MODIS snow cover data and a topography-based distribution function snowmelt model, Journal of Hydrology, 599, 126 020, https://doi.org/https://doi.org/10.1016/j.jhydrol.2021.126020, 2021.

Feng, X., Sahoo, A., Arsenault, K., Houser, P., Luo, Y., and Troy, T. J.: The Impact of Snow Model Complexity at Three CLPX Sites, Journal of Hydrometeorology, 9, 1464–1481, https://doi.org/10.1175/2008JHM860.1, 2008.

Gafurov, A. and Bárdossy, A.: Cloud removal methodology from MODIS snow cover product, Hydrology and Earth System Sciences, 13, 1361–1373, https://doi.org/10.5194/hess-13-1361-2009, 2009.

Girons Lopez, M., Vis, M. J. P., Jenicek, M., Griessinger, N., and Seibert, J.: Assessing the degree of detail of temperature-based snow routines for runoff modelling in mountainous areas in central Europe, Hydrology and Earth System Sciences, 24, 4441–4461, https://doi.org/10.5194/hess-24-4441-2020, 2020.

Hall, D., Salomonson, V., and Riggs, G.: MODIS/Terra Snow Cover 5-Min L2 Swath 500m, Version 5. Boulder, Colorado USA., NASA National Snow and Ice Data Center Distributed Active Archive Center, https://doi.org/10.5067/ACYTYZB9BEOS, 2006.

He, Z. H., Parajka, J., Tian, F. Q., and Blöschl, G.: Estimating degree-day factors from MODIS for snowmelt runoff modeling, Hydrology and Earth System Sciences, 18, 4773–4789, https://doi.org/10.5194/hess-18-4773-2014, 2014.

Hock, R.: A distributed temperature-index ice- and snowmelt model including potential direct solar radiation, Journal of Glaciology, 45, 101–111, https://doi.org/10.3189/S0022143000003087, 1999.

Hock, R.: Temperature index melt modelling in mountain areas, Journal of Hydrology, 282, 104–115, https://doi.org/https://doi.org/10.1016/S0022-1694(03)00257-9, mountain Hydrology and Water Resources, 2003.

Hofierka, J. and Suri, M.: The solar radiation model for Open source GIS: implementation and applications, Proceedings of the Open source GIS - GRASS users conference 2002, 2002.

Hudson, G. and Wackernagel, H.: Mapping temperature using kriging with external drift: Theory and an example from scotland, International Journal of Climatology, 14, 77–91, https://doi.org/https://doi.org/10.1002/joc.3370140107, 1994.

Jarvis, A., Guevara, E., Reuter, H., and Nelson, A.: Hole-filled SRTM for the globe : version 4 : data grid, published by CGIAR-CSI on 19 August 2008., 2008.

Kirkham, J. D., Koch, I., Saloranta, T. M., Litt, M., Stigter, E. E., Møen, K., Thapa, A., Melvold, K., and Immerzeel, W. W.: Near Real-Time Measurement of Snow Water Equivalent in the Nepal Himalayas, Frontiers in Earth Science, 7, 177, https://doi.org/10.3389/feart.2019.00177, 2019.

Martínez-Cob, A.: Multivariate geostatistical analysis of evapotranspiration and precipitation in mountainous terrain, Journal of Hydrology, 174, 19–35, https://doi.org/https://doi.org/10.1016/0022-1694(95)02755-6, 1996.

Neteler, M. and Mitasova, H.: Open source GIS: a GRASS GIS approach - Appendix, vol. 689, Kluwer Academic Pub, 2002.

Parajka, J. and Blöschl, G.: The value of MODIS snow cover data in validating and calibrating conceptual hydrologic models, Journal of Hydrology, 358, 240–258, https://doi.org/https://doi.org/10.1016/j.jhydrol.2008.06.006, 2008.

Parajka, J., Naeimi, V., Blöschl, G., and Komma, J.: Matching ERS scatterometer based soil moisture patterns with simulations of a conceptual dual layer hydrologic model over Austria, Hydrology and Earth System Sciences, 13, 259–271, https://doi.org/10.5194/hess-13-259-2009, 2009.

Phillips, D. L., Dolph, J., and Marks, D.: A comparison of geostatistical procedures for spatial analysis of precipitation in mountainous terrain, Agricultural and Forest Meteorology, 58, 119–141, https://doi.org/https://doi.org/10.1016/0168-1923(92)90114-J, 1992.

Riboust, P., Thirel, G., Moine, N. L., and Ribstein, P.: Revisiting a Simple Degree-Day Model for Integrating Satellite Data: Implementation of Swe-Sca Hystereses, Journal of Hydrology and Hydromechanics, 67, 70–81, https://doi.org/doi:10.2478/johh-2018-0004, 2019.

Rutter, N., Essery, R., Pomeroy, J., Altimir, N., Andreadis, K., Baker, I., Barr, A., Bartlett, P., Boone, A., Deng, H., Douville, H., Dutra, E., Elder, K., Ellis, C., Feng, X., Gelfan, A., Goodbody, A., Gusev, Y., Gustafsson, D., Hellström, R., Hirabayashi, Y., Hirota, T., Jonas, T., Koren, V., Kuragina, A., Lettenmaier, D., Li, W., Luce, C., Martin, E., Nasonova, O., Pumpanen, J., Pyles, R., Samuelsson, P., Sandells, M., Schädler, G., Shmakin, A., Smirnova, T., Stähli, M., Stöckli, R., Strasser, U., Su, H., Suzuki, K., Takata, K., Tanaka, K., Thompson, E., Vesala, T., Viterbo, P., Wiltshire, A., Xia, K., Xue, Y., and Yamazaki, T.: Evaluation of forest snow processes models (SnowMIP2), Journal of Geophysical Research, https://doi.org/10.1029/2008JD011063, 12.01.03; LK 01; 114(D06111), 2009, 2009.

Schaefli, B., Hingray, B., Niggli, M., and Musy, A.: A conceptual glacio-hydrological model for high mountainous catchments, Hydrology and Earth System Sciences, 9, 95–109, https://doi.org/10.5194/hess-9-95-2005, 2005.

Schmucki, E., Marty, C., Fierz, C., and Lehning, M.: Evaluation of modelled snow depth and snow water equivalent at three contrasting sites in Switzerland using SNOWPACK simulations driven by different meteorological data input, Cold Regions Science and Technology, 99, 27–37, https://doi.org/https://doi.org/10.1016/j.coldregions.2013.12.004, 2014.

Sirisena, T. A. J. G., Maskey, S., and Ranasinghe, R.: Hydrological Model Calibration with Streamflow and Remote Sensing Based Evapotranspiration Data in a Data Poor Basin, Remote Sensing, 12, https://doi.org/10.3390/rs12223768, 2020.

Sun, W., Ishidaira, H., Bastola, S., and Yu, J.: Estimating daily time series of streamflow using hydrological model calibrated based on satellite observations of river water surface width: Toward real world applications, Environmental Research, 139, 36–45, https://doi.org/https://doi.org/10.1016/j.envres.2015.01.002, environmental Research on Hydrology and Water Resources, 2015.

Tekeli, A. E., Akyürek, Z., Arda Şorman, A., Şensoy, A., and Ünal Şorman, A.: Using MODIS snow cover maps in modeling snowmelt runoff process in the eastern part of Turkey, Remote Sensing of Environment, 97, 216–230, https://doi.org/https://doi.org/10.1016/j.rse.2005.03.013, 2005.

Tran, H., Nguyen, P., Ombadi, M., lin Hsu, K., Sorooshian, S., and Qing, X.: A cloud-free MODIS snow cover dataset for the contiguous United States from 2000 to 2017, Sci Data, 6, https://doi.org/10.1038/sdata.2018.300, 2019.

Udnæs, H.-C., Alfnes, E., and Andreassen, L. M.: Improving runoff modelling using satellite-derived snow covered area?, Hydrology Research, 38, 21–32, 2007.

Wagner, W., Verhoest, N. E. C., Ludwig, R., and Tedesco, M.: Editorial "Remote sensing in hydrological sciences", Hydrology and Earth System Sciences, 13, 813–817, https://doi.org/10.5194/hess-13-813-2009, 2009.

Wang, X. and Xie, H.: New methods for studying the spatiotemporal variation of snow cover based on combination products of MODIS Terra and Aqua, Journal of Hydrology, 371, 192–200, https://doi.org/https://doi.org/10.1016/j.jhydrol.2009.03.028, 2009.